REPORT DOCUMENTATION PAGE

Form Approved
OMB No. 0704-0188

1a REPORT SECURITY CLASSIFICATION UNCLASSIFIED	1b. RESTRICTIVE MARKINGS
2a SECURITY CLASSIFICATION AUTHORITY	3. DISTRIBUTION / AVAILABILITY OF REPORT Approved for public release; distribution unlimited
2b DECLASSIFICATION / DOWNGRADING SCHEDULE	
4 PERFORMING ORGANIZATION REPORT NUMBER(S) PARGUM-87-04	5. MONITORING ORGANIZATION REPORT NUMBER(S)
6a. NAME OF PERFORMING ORGANIZATION Physical Acoustics Research Laboratory 6b. OFFICE SYMBOL (If applicable)	7a. NAME OF MONITORING ORGANIZATION Office of Naval Research
6c. ADDRESS (City, State, and ZIP Code) Department of Physics and Astronomy University, MS 38677	7b. ADDRESS (City, State, and ZIP Code) Physics Division, Code 1112 Arlington, VA 22217-5000
8a. NAME OF FUNDING / SPONSORING ORGANIZATION 8b. OFFICE SYMBOL (If applicable)	9. PROCUREMENT INSTRUMENT IDENTIFICATION NUMBER N00014-84-C-0193
8c. ADDRESS (City, State, and ZIP Code)	10. SOURCE OF FUNDING NUMBERS PROGRAM ELEMENT NO. 61153N11 / PROJECT NO. / TASK NO. 4126936 / WORK UNIT ACCESSION NO.

11 TITLE (Include Security Classification)

A Continued Study of Optical Sound Generation and Amplification

12 PERSONAL AUTHOR(S)
Bass, Henry E. and Shields, F. Douglas

13a TYPE OF REPORT	13b. TIME COVERED	14. DATE OF REPORT (Year, Month, Day)	15. PAGE COUNT
Annual	FROM 861001 TO 870930	31 October 1987	

16 SUPPLEMENTARY NOTATION

17 COSATI CODES			18. SUBJECT TERMS (Continue on reverse if necessary and identify by block number)
FIELD	GROUP	SUB-GROUP	Optoacoustics, Sound Amplification, Vibrational Energy Transfer, Nonequilibrium Acoustics

19 ABSTRACT (Continue on reverse if necessary and identify by block number)

During the past year, research has concentrated on optoacoustic generation in fluids, ultrasonic absorption in water/polymer mixtures, and sound propagation through a gas with a nonequilibrium distribution of internal energy states.

Preliminary optoacoustic measurements in water and propanol demonstrate that the theory explains experimental results for these weakly absorbing fluids. Attention then shifted to a strongly absorbing fluid with relaxing internal energy states, CS_2. Initial measurements in CS_2 reflect a non-linearity of signal strength with increasing input energy and the formation of visible bubbles near the optical focal point. A theoretical model for the optoacoustic signal as a function of time in the linear regime (energies too low for bubble formation) has been developed.

A new system to measure small absorption (~1 dB/m) in fluids in the frequency range 90 KHz to 1 MHz has been tested. Measurements in distilled water indicate that

20 DISTRIBUTION / AVAILABILITY OF ABSTRACT ☒ UNCLASSIFIED/UNLIMITED ☐ SAME AS RPT. ☐ DTIC USERS	21. ABSTRACT SECURITY CLASSIFICATION UNCLASSIFIED
22a NAME OF RESPONSIBLE INDIVIDUAL Logan E. Hargrove	22b. TELEPHONE (Include Area Code) (202) 696-4221 22c. OFFICE SYMBOL ONR Code 1112

DD Form 1473, JUN 86 *Previous editions are obsolete.* SECURITY CLASSIFICATION OF THIS PAGE

A CONTINUED STUDY OF OPTICAL SOUND GENERATION AND AMPLIFICATION

Henry E. Bass and F. Douglas Shields

Physical Acoustics Research Laboratory
University of Mississippi
University, Mississippi 38677
PARGUM 87-4

29 October 1987

Annual Report
ONR Contract N00014-84-C-0193

Approved for public release;
distribution unlimited

Prepared for:

OFFICE OF NAVAL RESEARCH
DEPARTMENT OF THE NAVY
ARLINGTON, VIRGINIA 22217

Table of Contents

1.0 Optoacoustic Studies of Liquids

1.1 Introduction

Investigations of optoacoustic generation in liquids are well documented.[1,2,3] Most of these studies were carried out using low optical energies and small optical absorption coefficients. A small optical absorption coefficient makes the symmetry of the problem simple; the mathematics tractable. In the low optical energy regime, the acoustic generation mechanism is thermal expansion. This is the basis for linear optoacoustic theory. Nonlinear effects occur when the liquid experiences multiphoton absorption or a phase transition.

On a molecular level, the optoacoustic effect can be broken down into several different steps. The process of converting optical energy to acoustical energy begins with the absorption of photons by the molecules of the fluid. This absorption leaves the molecules in an excited state. In the present case, a nitrogen laser, used as the energy source, produces electronic excitation of the molecules. Dissipation of this energy can occur through several mechanisms including; photochemical processes, radiative decay, and nonradiative decay. In nonradiative decay, the electronic excitation energy is transferred to translational, rotational or vibrational states of the molecule. Through interactions with other molecules this rotational and vibrational energy can be converted into translational energy creating a temperature rise in the fluid. In our experiment, following each pulse from the laser, the fluid is allowed to cool to an ambient temperature. This alternate heating and cooling creates a pressure variation which is observed as acoustic pulses.

Present optoacoustic theories[4,5,6] assume that the energy transfer processes discussed above all take place over a period of time which is very short compared to other factors that effect the observed pressure profile; such as, the length of the laser pulse and its diameter as it enters the fluid.

The process of energy transfer and the rate at which it occurs varies from one liquid to another because the energy levels and rate of energy transfer depend on the structure of the

molecules. If the rate of production of translational energy is slow due to internal relaxation processes, the shape of the acoustic pulse should be governed by these relaxation processes. The experimental system must be capable of resolving very short acoustic pulses in order to resolve events occuring on this time scale. Otherwise, the pressure profile is dominated by geometrical factors of the experiment.

Carbon disulfide (CS_2) has been chosen as one subject of study because previous ultrasonic absorption measurements[7] have already shown that the transfer of energy between translational and vibrational states is relatively slow (compared, for example, to H_2O). This transfer of energy into translation can be described by a relaxation equation which gives rise to an exponetial decay in the number of excited molecules. Since some of the energy will go directly from electronic to translation, it is expected that the optoacoustic signal in CS_2 will be a simple superposition of such an exponential decay and a signal such as occurs in liquids where the energy transfer takes place much more quickly. By extracting this exponential decay process from the raw data, we can determine the relaxation time that characterizes the energy transfer process.

One can view a liquid as being composed of dynamic molecular groups referred to as clusters.[7] The average number of molecules per cluster differs for various fluids. Photons absorbed by these clusters cause a redistribution or reorientation of the molecules which results in a change in density. These molecular movements result in an outwardly spreading acoustic wave. By monitoring characteristics such as amplitude, relaxation time, and the shape of the wave, one might be able to gain insight to the molecular dynamics of the system. For example, a state of increasing instability is expected with increasing photon density. As N_p (the number of photons absorbed per unit volume in one relaxation time) surpasses the number of clusters (N_c), clusters begin to break up to a greater extent until the liquid vaporizes. As the system nears this regime, quantities characteristic of the liquid state approach those of the gaseous state. It is near this phase transition that the established linear theory is no longer applicable.

Experimental Configuration

A block description of the experimental technique is shown in Figure 1.1. This technique utilizes two lasers. A 1.25 MW nitrogen laser emitting 800 ps pulses in the UV (337 nm) is used as the optoacoustic source. A 3mW continuous He-Ne laser runs parallel to the excitation zone. It is then focused on a photodiode which is coupled to a digitizing oscilloscope. The probe laser responds to refractive index gradients which are produced as a result of the acoustic wave. These gradients cause small deflections of the probe beam which are detected by the photodiode. The observed signal is proportional to the pressure gradient. Comparison to theory can be achieved by either integrating the observed signal or by differentiating the predicted pressure. Both techniques have been used; however, a comparison to the absolute magnitude of the acoustic pressure can be achieved as well if the theory is compared to the output of a PVDF hydrophone as shown in Figure 1.2. Given the inaccuracies in beam size estimates, the agreement between theory and experiment is considered acceptable.

Energy delivered to the fluid is varied by placing glass slides in the beam path of the UV laser. N number of glass slides (~ .23 mm thick) are supported by two small pieces of plexiglass. The centers of the plexiglass have been removed. To provide for accurate energy measurements, twenty sets of attenuators corresponding to a different number of glass slides were made. The energy transmission for each attenuation was measured with an energy meter. The precision of the energy meter is $\pm$ 1μJ. Figure 1.3 shows measured energy delivered to the test cell as a function of the number of glass slides.

The energy density in the fluid can also be increased by increasing the optical absorption coefficient α. This is achieved by either adding dye to the test liquid or by choosing a liquid that strongly absorbs UV radiation.

1.2 Initial Studies Near the Non-Linear Regime

In optoacoustical studies on the molecular level, among the parameters that must be determined are the number of fluid molecules being excited and the number of photons being

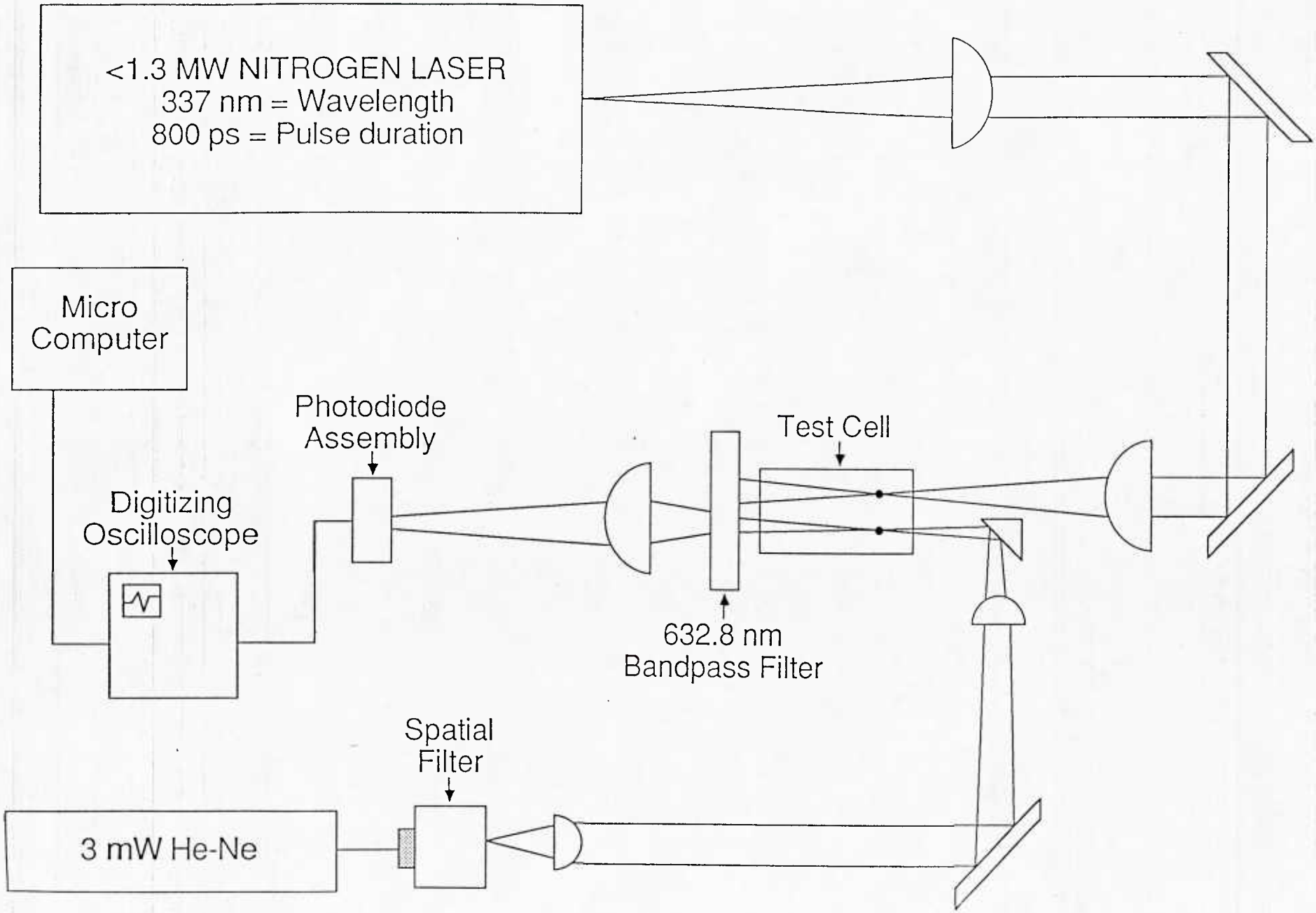
<1.3 MW NITROGEN LASER
337 nm = Wavelength
800 ps = Pulse duration
Micro Computer
Photodiode Assembly
Test Cell
Digitizing Oscilloscope
632.8 nm Bandpass Filter
Spatial Filter
3 mW He-Ne

Figure 1.1

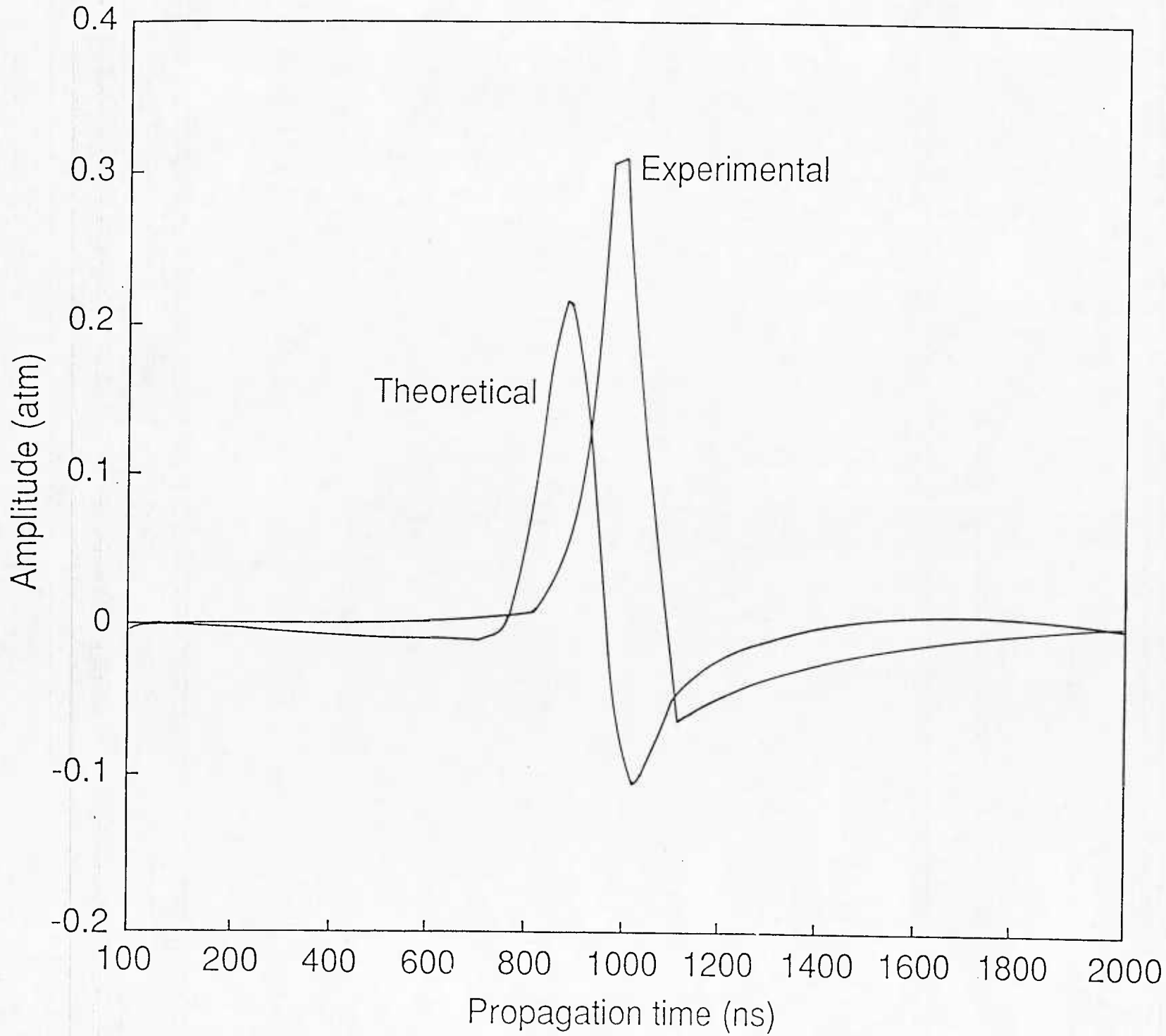
0.4
0.3
0.2
0.1
0
-0.1
-0.2
Amplitude (atm)
Experimental
Theoretical
100
200
400
600
800
1000
1200
1400
1600
1800
2000
Propagation time (ns)

Figure 1.2

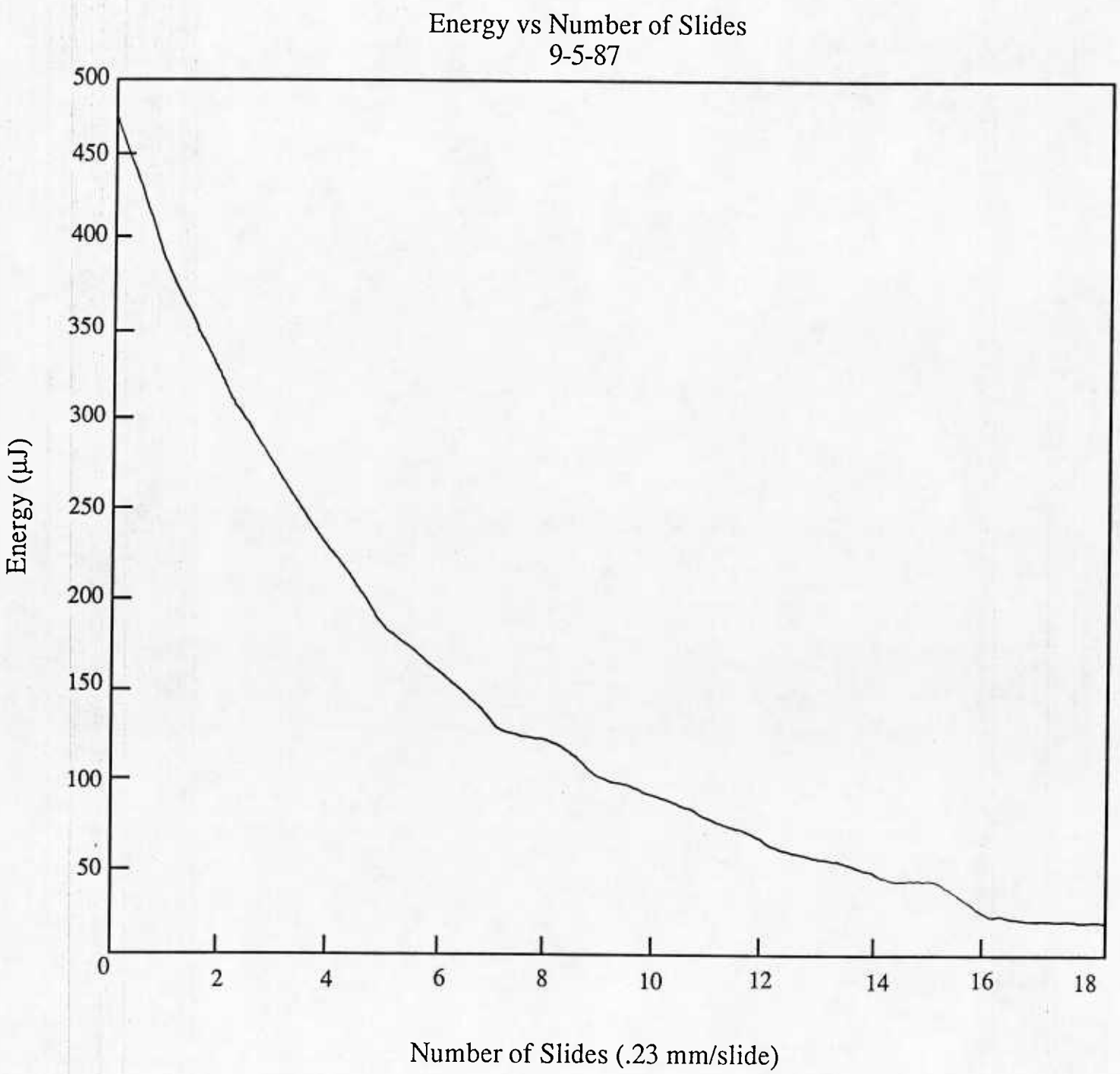
Energy vs Number of Slides
9-5-87
Energy (µJ)
500
450
400
350
300
250
200
150
100
50
0
2
4
6
8
10
12
14
16
18
Number of Slides (.23 mm/slide)

Figure 1.3

absorbed per unit time. The number of photons is easily obtained by measuring the total energy of the pulse with an energy meter and dividing by the energy per photon. The number of molecules is obtained by first measuring the optical absorption coefficient α of the liquid. The optical penetration depth is then the reciprocal of α. Knowing the laser beam dimensions and assuming exponential decay, one can then find the excitation volume.

The optical absorption coefficient of pure CS_2 at $\lambda = 337$ nm is large. To measure α, small amounts of CS_2 were added to propanol which has a much smaller absorption coefficient. The energy passing entirely through the test cell, measured by an energy meter, is then

$$E = E_o e^{-\left[(1-f)\alpha_1 + f\alpha_2\right]x - a} \quad \text{where} \tag{1.1}$$

α_1 = absorption coefficient of pure propanol and the test cell

α_2 = absorption coefficient of pure CS_2

a = absorption of the test cell

f = fraction of CS_2 in propanol, and

x = length of test cell (4 cm).

In all cases of interest, f and a are very small so $\alpha_1(1-f)x + a \cong \alpha_1 x$. The quantity $\alpha_1 x$ can be measured by first measuring the energy, E_{max}, in the absence of the test cell and then the energy, E_o, when the test cell full of propanol is placed in the beam path. We then have

$$E_o = E_{max} e^{-\alpha_1 x}. \tag{1.2}$$

For our system, E_{max} was found to be 0.363 mJ and E_o was found to be 0.340 mJ so $\alpha_1 x = 0.0655$. We now can write Eq. (1.1) as

$$E = E_o e^{-0.0655} e^{-f\alpha_2}. \tag{1.3}$$

The total volume V of propanol for this experiment was 12 mL. Drops of CS_2 with a volume of 0.01 ml were added to the propanol so that

$$f = \frac{N \cdot (.01)}{12} \tag{1.4}$$

where N is the number of drops. Energy transmission was measured after each drop. From this data α_2 was deduced to be 370 cm^{-1} which implies a penetration depth for pure CS_2 of 27μm.

The excitation volume is then given by

$$V = xy \int_0^\infty e^{-\alpha_2 z} dz \qquad \text{where} \tag{1.5}$$

x and y are the spatial dimensions of the rectangular laser pulse. From the measured values of x, y, and α_2 we obtain B = 2.22 x $10^{-6} cm^3$.

The number of molecules n, in the excitation volume is

$$n = \frac{\rho V N}{W} \qquad \text{where} \tag{1.6}$$

ρ = density of CS_2 = 1.263 g/cm^3

N = Avagadro's number

W = molecular weight of CS_2

From these values, the excitation volume contains 2.22 x 10^{16} CS_2 molecules.

A nonlinear transition has been observed in CS_2 when sufficient energy density is applied. We now refer to Figure 1.4 which is a plot of acoustic amplitude vs laser pulse energy in CS_2. There are three regimes of interest on this curve which are separated by two regions of constant acoustic amplitude. The first extends from zero to 75 μJ. The boiling point of CS_2 is 46° C. The equilibrium temperature of the liquid was 22° C. In order to achieve the boiling point, a temperature rise of 24° C is required. Knowing the specific heat and the mass of the fluid, one can determine the laser pulse energy required to achieve the boiling point. The boiling point, bp, is indicated near this first plateau. The second regime extends from 90 μJ to 160 μJ. The slope of the second regime increases relative to the first indicating a higher optoacoustic conversion efficiency probably due to vaporization of the

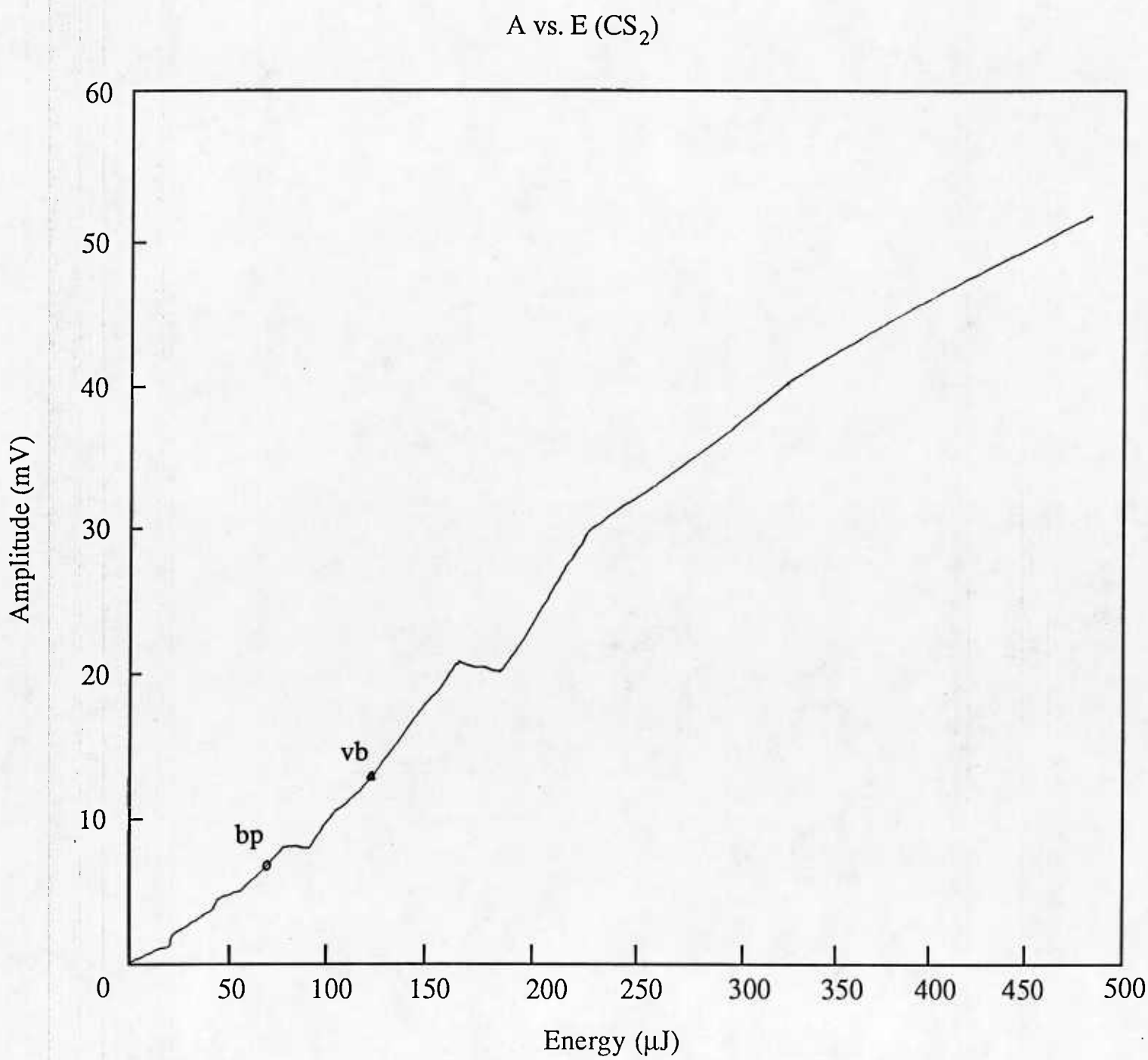
A vs. E (CS_2)
Amplitude (mV)
60
50
40
30
20
10
0
50
100
150
200
250
300
350
400
450
500
Energy (μJ)
vb
bp

Figure 1.4

liquid. The point where vaporization bubbles appeared to the unaided eye is indicated by vb. The third regime extends from 190 μJ to E_{max}. The slope changes again indicating optical saturation of the liquid.

1.3 Opto-Acoustic Observations in a Relaxing Fluid

Ultimately we wish to use the optoacoustic effect to investigate relaxation processes in fluids. For most fluids, internal reorientations take place very rapidly, much faster than the present experimental apparatus can resolve. As an interim step, fluids with relatively slow internal relaxations will be explored. The prototype for such behavior is CS_2. Ultrasonic attenuation measurements have shown that liquid CS_2 has a very slow internal relaxation.[8]

For relaxation measurements, nonlinearity is undesirable so a sufficient number of glass slides were placed between the excitation laser and the CS_2 test cell to insure operation in the linear regime. Even in the linear regime, the large absorption coefficient presents difficulties. Specifically, since the excitation energy is all absorbed within a depth not much different in size from the laser beam waist, the source for the optoacoustic signal appears more spherical than cylindrical. The more complex geometry results in theoretical expressions which are much more complex than those used by previous investigators.[6]

Experimental Results

Prior to launching into a tedious mathematical derivation, it is of interest to examine the general shape of the experimental curves. Figure 1.5 shows the magnitude of the probe beam deflection versus time for propanol. Hutchins and Tam [2] found this same general shape for other fluids as well. In this case, energy is transferred to the fluid more rapidly than the experimental apparatus can respond so the waveform is dictated by laser beam geometries.

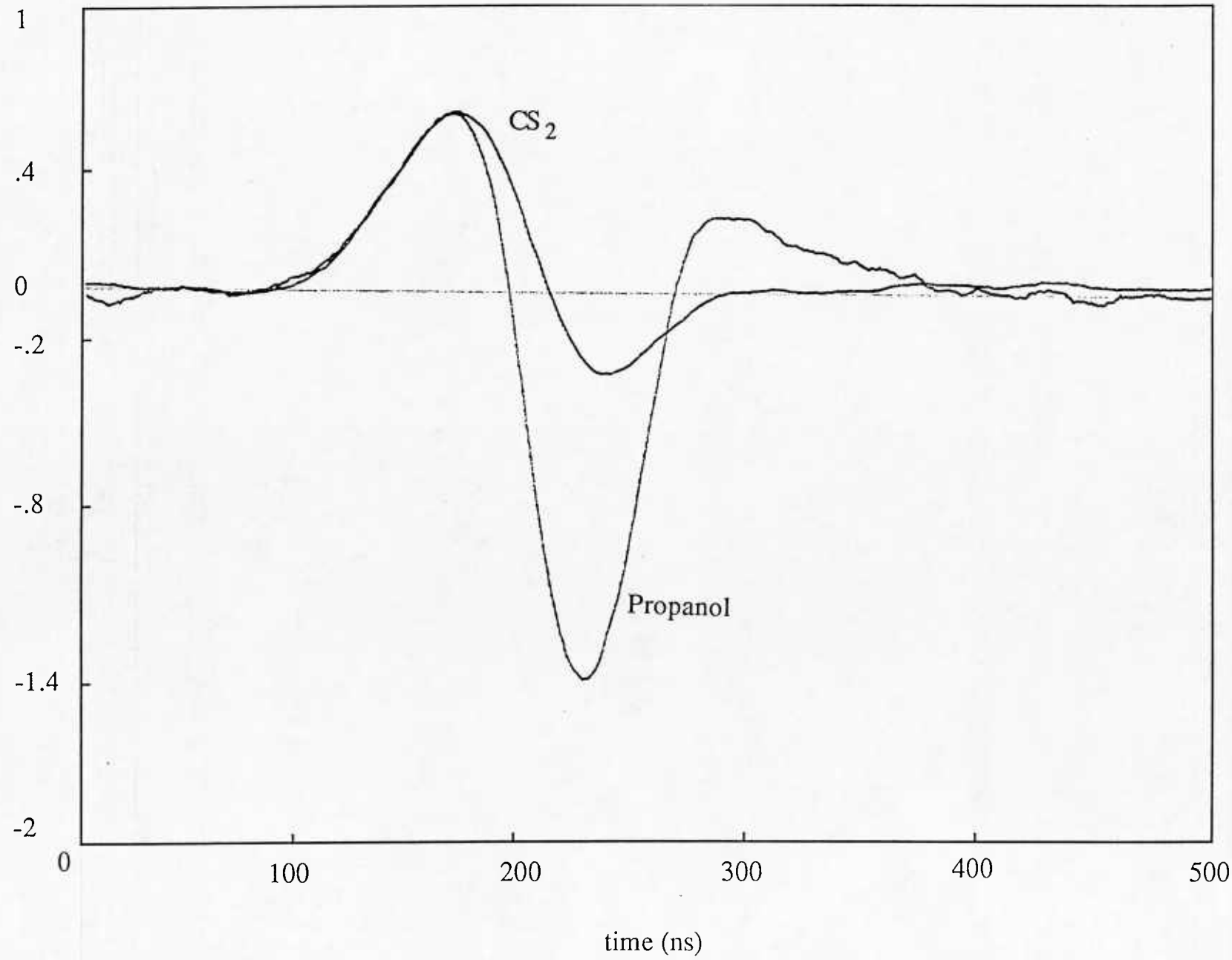
1
.4
0
-.2
-.8
-1.4
-2
0
100
200
300
400
500
CS 2
Propanol
Relative Amplitude
time (ns)

Figure 1.5

11

Also shown in Figure 1.5 is a wave form observed under similar conditions for CS_2. Note that although the rise time is comparable to that for propanol, the decay is much slower and the waveform spends much more time positive. It is not yet clear whether this behavior is a result of a slowly relaxing internal mode or the much larger optical absorption in CS_2 which leads to a more spherical source term.

Relaxation Equations

Assume that the incoming laser beam is radially Gaussian with a beam waist **a**, with a Gaussian time dependence characterized by t_p, and is absorbed in accordance with Beer's law,[9] then the intensity I can be written as

$$I(r,z,t) = \frac{I_o\sqrt{e}}{t_p}\, t\, \exp\left(\frac{-r^2}{a^2} - \alpha z - \frac{t^2}{t_p^2}\right). \tag{1.7}$$

The energy absorbed per unit time per unit volume by the fluid is

$$w(r,z,t) = \alpha I(r,z,t) \tag{1.8}$$

but this is not the energy which appears in translation per unit time. This fact makes our treatment different from previous ones. We will assume that only when the energy appears in translation is there a change in density. In fact, an increase in electronic or vibrational states could lead to density changes through variations in bond lengths or intermolecular bonding, but these will be ignored for now.

For simplicity, consider a three level system as shown below.

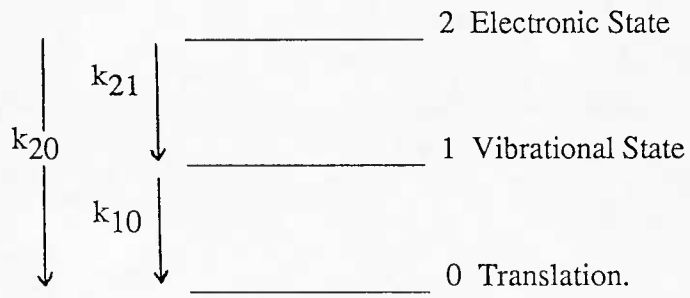

Following the notation of Bauer,[10] we introduce a set of progress variables, ξ_α such that

$$\dot{\xi}_\alpha = n(k_\alpha x_i x_j - k_\alpha' x_k x_l) \tag{1.9}$$

where α refers to an energy transfer reaction, i - l refer to initial and final states of collision pairs, and k_α and k_α' are forward and reverse reactions respectively. In this notation, the change in fluid translational energy is given by

$$\dot{E}_\alpha = \dot{\xi}_\alpha \Delta E_\alpha \tag{1.10}$$

where ΔE_α is the energy deficit in reaction α.

It should be noted at this point that in a fluid, ternary collisions as well as unimolecular reactions might be important. These can be handled with pseudoreactions of the above type provided we are always operating at the same liquid density.

At equilibrium,

$$k_\alpha^o x_i^o x_j^o - k_\alpha'^o x_k^o x_l^o = 0 . \tag{1.11}$$

If we expand near equilibrium,

$$\dot{\xi}_\alpha / n = k_\alpha^o x_i^o x_j^o + \frac{\partial k_\alpha x_i x_j}{\partial T} dT + \sum_m \frac{\partial k_\alpha' x_i x_j}{\partial n_m} dn_m$$

$$-k_\alpha^{o'} x_k^o x_l^o - \frac{\partial k_\alpha x_k x_l}{\partial T} dT - \sum_m \frac{\partial k_\alpha x_k x_l}{\partial n_m} dn_m . \tag{1.12}$$

Note that k_α depends upon T not n_m while x's depend upon n_m,

$$-k_\alpha = k_\alpha' e^{-\Delta E_d/RT}, \tag{1.13}$$

and

$$x_i = \frac{n_i}{n}. \tag{1.14}$$

We can then write

$$\frac{\partial k_\alpha x_i x_j}{\partial T} dT = k_\alpha x_i^o x_j^o \frac{\partial \ln k_\alpha}{\partial T} dT \text{ , etc.} \tag{1.15}$$

so

$$\dot{\xi}_\alpha / n = k_\alpha^o x_i^o x_j^o \left[\left(\frac{\partial \ln k_\alpha}{\partial T} - \frac{\partial \ln k_\alpha'}{\partial T} \right) \right] + k_\alpha^o x_i^o x_j^o \sum_m \left(\frac{\partial \ln x_i x_j}{\partial n_m} - \frac{\partial \ln x_k x_l}{\partial n_m} \right) dn_m \tag{1.16}$$

or

$$\dot{\xi}_\alpha / n = k_\alpha^o x_i^o x_j^o \left[\frac{\partial}{\partial T} \ln(k_\alpha / k_\alpha')(T - T_o) \right] + \sum_m \left\{ \left(\frac{\partial \ln x_i}{\partial n_m} + \frac{\partial \ln x_j}{\partial n_m} - \frac{\partial \ln x_k}{\partial n_m} - \frac{\partial \ln x_l}{\partial n_m} \right) \left(n_m - n_m^o \right) \right\} \tag{1.17}$$

or

$$\dot{\xi}_\alpha / n = k_\alpha^o x_i^o x_j^o \left\{ \frac{\partial}{\partial T} \left(-\frac{\Delta E_\alpha}{RT} \right) \left(T - T^o \right) + \sum_m \frac{\partial \ln n_i}{\partial n_m} + \frac{\partial \ln n_j}{\partial n_m} \ldots \right\}. \tag{1.18}$$

Any dependence of n_i on n_m is explicit except for m = i. So

$$\sum_m \frac{\partial \ln n_i}{\partial n_m}\left(n_m - n_m^o\right) = \frac{n_i - n_i^o}{n_i}, \text{ etc.} \tag{1.19}$$

With this observation included,

$$\dot{\xi}_\alpha/n = k_\alpha^o x_i^o x_j^o \left\{ \frac{\Delta E_\alpha}{RT^2}\left(T - T^o\right) + \frac{n_i - n_i^o}{n_i} + \frac{n_j - n_j^o}{n_j} - \frac{n_l - n_l^o}{n_l} - \frac{n_k - n_k^o}{n_k} \right\}. \tag{1.20}$$

We are interested in reactions of the form

$$m_i + m_j \overset{k_\alpha}{\leftrightarrow} m_l + m_j + \Delta E_\alpha,$$

that is, j = k, so the process takes place at the same rate no matter what the collision partners. Since our reactions may be unimolecular, this form is especially desirable since now,

$$\dot{\xi}_\alpha/n = k_\alpha^o x_i^o x_j^o \left\{ \frac{\Delta E_\alpha}{RT^2}\left(T - T^o\right) + \frac{n_i - n_i^o}{n_i} - \frac{n_l - n_l^o}{n_l} \right\}. \tag{1.21}$$

We are dealing with three reactions,

$$\dot{\xi}_1 = k_{1o} x_1^o x_o^o \left\{ \frac{\Delta E_1}{RT^2}\left(T - T_o\right) + \frac{n_1 - n_1^o}{n_1} - \frac{n_o - n_o^o}{n_o} \right\}, \tag{1.22a}$$

$$\dot{\xi}_2 = k_{2o} x_2^o x_o^o \left\{ \frac{\Delta E_2}{RT^2}\left(T - T_o\right) + \frac{n_2 - n_2^o}{n_2} - \frac{n_o - n_o^o}{n_o} \right\}, \tag{1.22b}$$

and

$$\dot{\xi}_3 = k_{21} x_2^o x_1^o \left\{ \frac{\Delta E_{12}}{RT^2}\left(T - T^o\right) + \frac{n_2 - n_2^o}{n_2} - \frac{n_1 - n_1^o}{n_1} \right\}. \tag{1.22c}$$

From these equations, one can solve for relaxation times, τ_1 and τ_2 and relaxation strengths, A_1 and A_2 which completely describe the transfer of energy to translation. Actually, one other equation is needed,

$$n = n_o + n_1 + n_2 \tag{1.23}$$

and A_1 and A_2 depend upon the excitation source. Solutions of this equation will be left for later.

Wave Equation

The inhomogenous wave equation for acoustic pressure, ignoring electrostriction, can be written [according to Eq. (15) of Ref. 2] as

$$\left(\frac{1}{c^2}\frac{\partial^2}{\partial t^2} - \nabla^2\right) p = \frac{\alpha\beta}{C_p}\frac{\partial}{\partial t} I(r,z,t) \tag{1.24}$$

where c is the speed of sound, α is the optical attenuation coefficient, β is the expansion coefficient, C_p is the specific heat and I is the source intensity. We can make use of this equation if we recognize that αI is the rate of energy deposition per unit volume which, in our case ($\tau_{\text{laser pulse}} << \tau_{\text{relaxation}}$) is controlled by energy transfer (relaxation).

Since t_p (same as $\tau_{\text{laser pulse}}$) is very small, we will rewrite the equation for intensity as

$$I(r,z,t) = \left[A_{1/\tau_1} e^{-t/\tau_1} + A_{2/\tau_2} e^{-t/\tau_2}\right] e^{-r^2/a^2} e^{-\alpha z}. \tag{1.25}$$

This is no longer the laser intensity but, rather, is the laser intensity modified for the time required for energy transfer. Normalizing,

$$E_p(\text{energy in pulse}) = \int I(r',z',t')\, r'dr'd\theta'dt' \tag{1.26}$$

or

$$E_p = \int_0^{\infty} (A_{1/\tau_1} e^{-t'/\tau_1}) + e^{-r'^2/a^2} r'dr'd\theta'dt' + \text{like terms for } \tau_2. \tag{1.27}$$

Integrating over all time and space,

$$E_p = \pi a^2 (A_1 + A_2) \Rightarrow A_2 = \frac{E_p}{\pi a^2} - A_1. \tag{1.28}$$

It is sometimes convenient to introduce a scalar potential, ϕ, at this point such that

$$\left(\frac{1}{c^2}\frac{\partial^2}{\partial t^2} - \nabla^2\right)\phi = I(r,z,t) \tag{1.29}$$

and

$$p = \frac{\alpha\beta}{C_p}\frac{\partial\phi}{\partial t} \tag{1.30}$$

then

$$\left[\frac{1}{c^2}\frac{\partial^2}{\partial t^2} - \nabla^2\right]\phi = A_{2/\tau_2}\left[\frac{\tau_2 A_1}{\tau_1 A_2} e^{-t/\tau_1} + e^{-t/\tau_2}\right] e^{-r^2/a^2} e^{-\alpha z}. \tag{1.31}$$

This inhomogeneous wave equation can be solved using Green's functions. The general form is

$$\nabla^2\psi - \frac{1}{c^2}\frac{\partial^2\psi}{\partial t^2} = -4\pi q(\vec{r},t) \tag{1.32}$$

in which case

$$\psi(\vec{r},t) = \frac{1}{4\pi}\int dV_o \frac{q(\vec{r_o},\, t\text{-}R/c)}{R} \tag{1.33}$$

where

$$R = \left[(x\text{-}x_o)^2 + (y\text{-}y_o)^2 + (z\text{-}z_o)^2 \right]^{1/2}. \tag{1.34}$$

If we transform to cylindrical coordinates,

$$x = r\cos\theta \qquad y = r\sin\theta \qquad z = z$$

$$R = \sqrt{r^2 + r_o^2 - 2rr_o\cos(\theta-\theta_o) + (z-z_o)^2} \qquad dV_o = r_o dr_o d\theta_o dz_o \quad \text{so}$$

$$\phi(r,t) = \frac{1}{4\pi}\int dV_o \cdot \frac{\dfrac{A_2}{4\pi\tau_2}\left[\dfrac{A_1\tau_2}{A_2\tau_1} e^{-(t-R/c)/\tau_1} + e^{-(t-R/c)/\tau_2}\right] e^{-r_o^2/a^2} e^{-\alpha z_o}}{R}$$

or

$$\phi(r,t) = \frac{A_2}{\tau_2(4\pi)^2}\int dV_o \frac{\left[\dfrac{\tau_2}{\tau_1}\dfrac{A_1}{A_2} e^{-(t-R/c)/\tau_1} + e^{-(t-R/c)/\tau_2}\right] e^{-r_o^2/a^2} e^{\alpha z_o}}{R} \tag{1.35}$$

and

$$p = \frac{\alpha\beta}{(4\pi)^2 C_p} \frac{A_2^2}{\tau_2^2} \int dV_o \frac{\left[\frac{-A_1^2 \tau_2^2}{A_2^2 \tau_1^2} e^{-(t-R/c)/\tau_1} - e^{-(t-R/c)/\tau_2} \right] e^{-r_o^2/a^2} e^{-\alpha z_o}}{R}.$$

We measure $\partial n(r,t)/\partial r$ or, if we assume $n \propto \rho \propto p$, then $\partial n(r,t)/\partial r$ is proportional to

$$\frac{\partial p}{\partial r} = \frac{\alpha\beta}{(4\pi)^2 C_p} \frac{A_2^2}{\tau_2^2} \int dV_o \left[\frac{A_1^2 \tau_2^2}{A_2^2 \tau_1^2} \left\{ \frac{e^{-(t-R/c)/\tau_1}}{R^3} - \frac{e^{-(t-R/c)/\tau_1}}{c\tau_1 R^2} \right\} \right.$$

$$\left. + \left\{ \frac{e^{-(t-R/c)/\tau_2}}{R^3} - \frac{e^{-(t-R/c)/\tau_2}}{R^2} \right\} \right] \left\{ r - r_o \cos(\theta - \theta_o) \right\} e^{-r_o^2/a^2} e^{-\alpha z_o}.$$

Current Status

At this time, we have observed an optoacoustic signal in CS_2. The optoacoustic signal is quite different from that observed in propanol. Mathematical equations taking into account relaxation and strong optical absorption have been derived and programmed. We are now in the process of comparing experimental results to these calculations. This investigation will comprise an M.S. thesis by Mr. Charles Thompson with an expected completion date of 15 December 1987.

References

1. P.J. Westervelt and R.S. Larson, "Laser-excited broadside array," J. Acoust. Soc. Am. 54, 121 (1973).

2. D.A. Hutchins and A.C. Tam, "Pulsed photoacoustic materials characterization," IEEE Transactions on Ultrasonics, Ferroelectronics and Frequency Control, Vol. UFFC-33 No. 5 Sept. 1986.
3. A.C. Tam, "Applications of photoacoustic sensing techniques," Rev of Modern Physics, Vol. 58, No. 2, 381, April 1986.
4. Y.H. Berthelot and I. J. Busch-Vishniac, "Laser-induced thermoacoustic radiation," J. Acoust. Soc. Am. 78, 2074 (1985).
5. B. Sullivan and A.C. Tam, "Profile of laser-produced acoustic pulse in a liquid," J. Acoust. Soc. Am. 75, 437 (1984).
6. H.M. Lai and K. Young, "Theory of the pulsed optoacoustic technique," J. Acoust. Soc. Am. 72, 2000 (1982).
7. Hirschfelder, Curtiss, and Bird, "Molecular Theory of Gases and Liquids," (John Wiley & Sons, Inc., New York, London), p. 375.
8. J.H. Andreae, E.L. Heasell and J. Lamis, "Ultrasonic relaxation and the vibrational specific heat of carbon disulfide," Proc. Phys. Soc. B69, 625 (1956).
9. G.S. Bushanam, F.S. Barnes, "Laser-generated thermoelastic shock wave in liquids," J. Appl. Phys. 46, 2074 (1975).
10. Hans-Jorg Bauer, "Son et lumiere or the optoacoustic effect in multilevel systems," J. Chem. Phys. 57, 3130 (1972).

2.0 Ultrasonic Attenuation in Polymer /Water Mixtures

During the period 1 May, 1985 - 30 September, 1985 in cooperation with Professor John Jacobus at Tulane and with support by the Naval Oceanographic Research and Development Activity ultrasonic attenuation was measured in a variety of aqueous polymer solutions.[1] This initial study identified three polymers as having significant attenuation in excess of that for pure water. These were Polyethylene Oxide (MW = 14,000), Polycoethylene Glycol (MW = 15,000), and Hexadecyl trimethyl ammonium bromide. All showed excess attenuation near 2.5 dB/m at some frequencies, but the 14K PEO showed the maximum attenuation at 630 KHz.

The ultrasonic apparatus used in the preliminary study was restricted to a range 0.63 MHz to 2.5 MHz with an absolute accuracy of approximately 1.0 dB/m. Though this accuracy was acceptable at the time since our goal was to screen solutions for those having an excess attenuation of 10 dB/m, the frequency range was not sufficient to identify mechanisms. These preliminary measurements illustrated that a solution with good attenuation at high frequency (CTAB at 1.6 MHZ) might show almost no attenuation at lower frequencies (630 KHz) which is suggestive of a relaxation process. The reverse is also true (14K PEO for example).

In the past few months, an ultrasonic apparatus designed to operate at lower frequencies was assembled and tested. This apparatus was originally proposed for the initial work but delays in funding prompted us to go with an available instrument instead of the optimum system.

2.1 Ultrasonic Apparatus

The ultrasonic apparatus to be used for chemically-induced ultrasound attenuation measurements (Figures 2.1-2.3) consists of sending and receiving transducers separated by a variable distance, Δx. The transmitting transducer is driven by an amplified tone burst

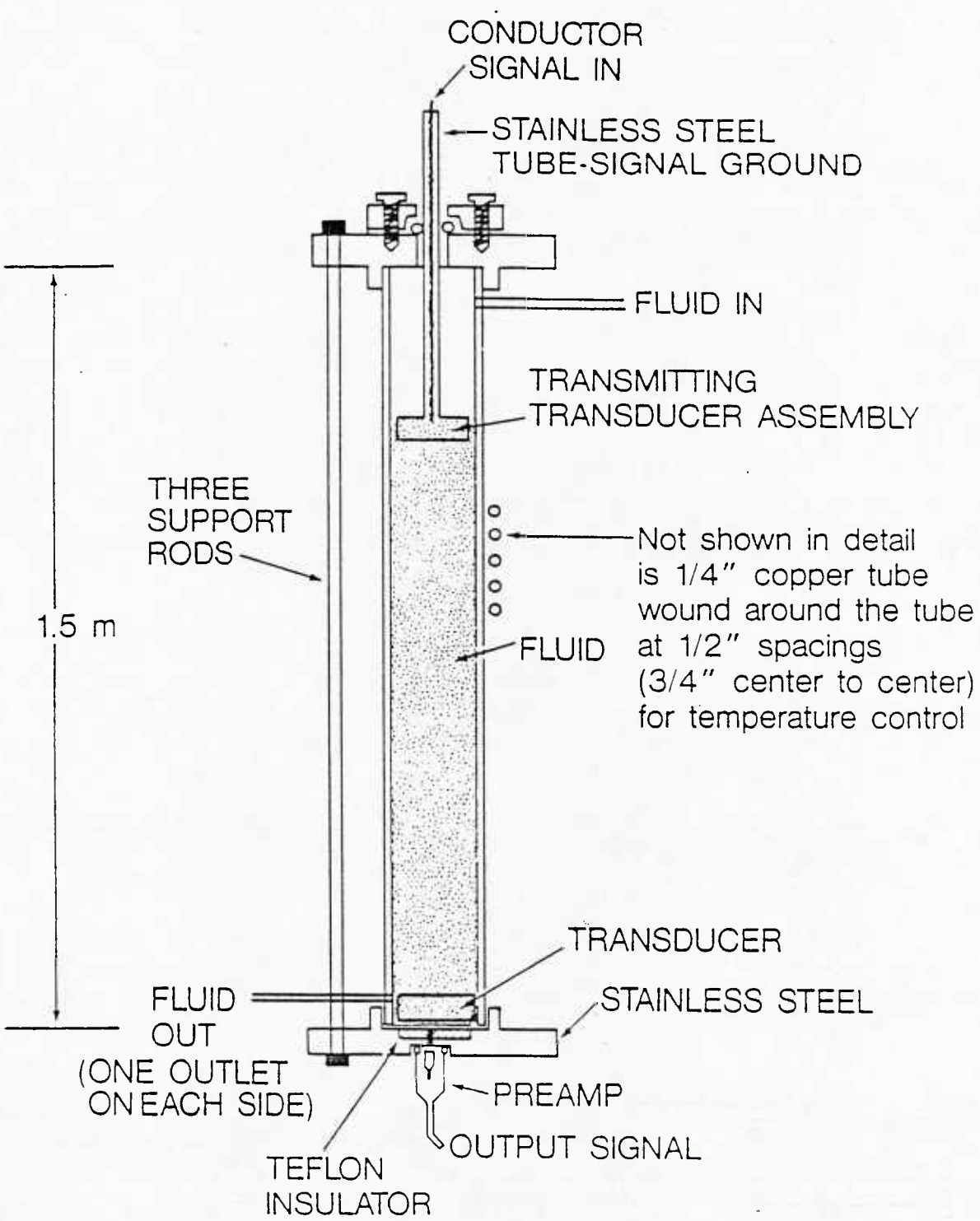
ULTRASONIC APPARATUS
CONDUCTOR
SIGNAL IN
STAINLESS STEEL
TUBE-SIGNAL GROUND
FLUID IN
TRANSMITTING
TRANSDUCER ASSEMBLY
THREE
SUPPORT
RODS
Not shown in detail
is 1/4" copper tube
wound around the tube
at 1/2" spacings
(3/4" center to center)
for temperature control
1.5 m
FLUID
TRANSDUCER
FLUID
OUT
(ONE OUTLET
ON EACH SIDE)
STAINLESS STEEL
PREAMP
OUTPUT SIGNAL
TEFLON
INSULATOR

Figure 2.1

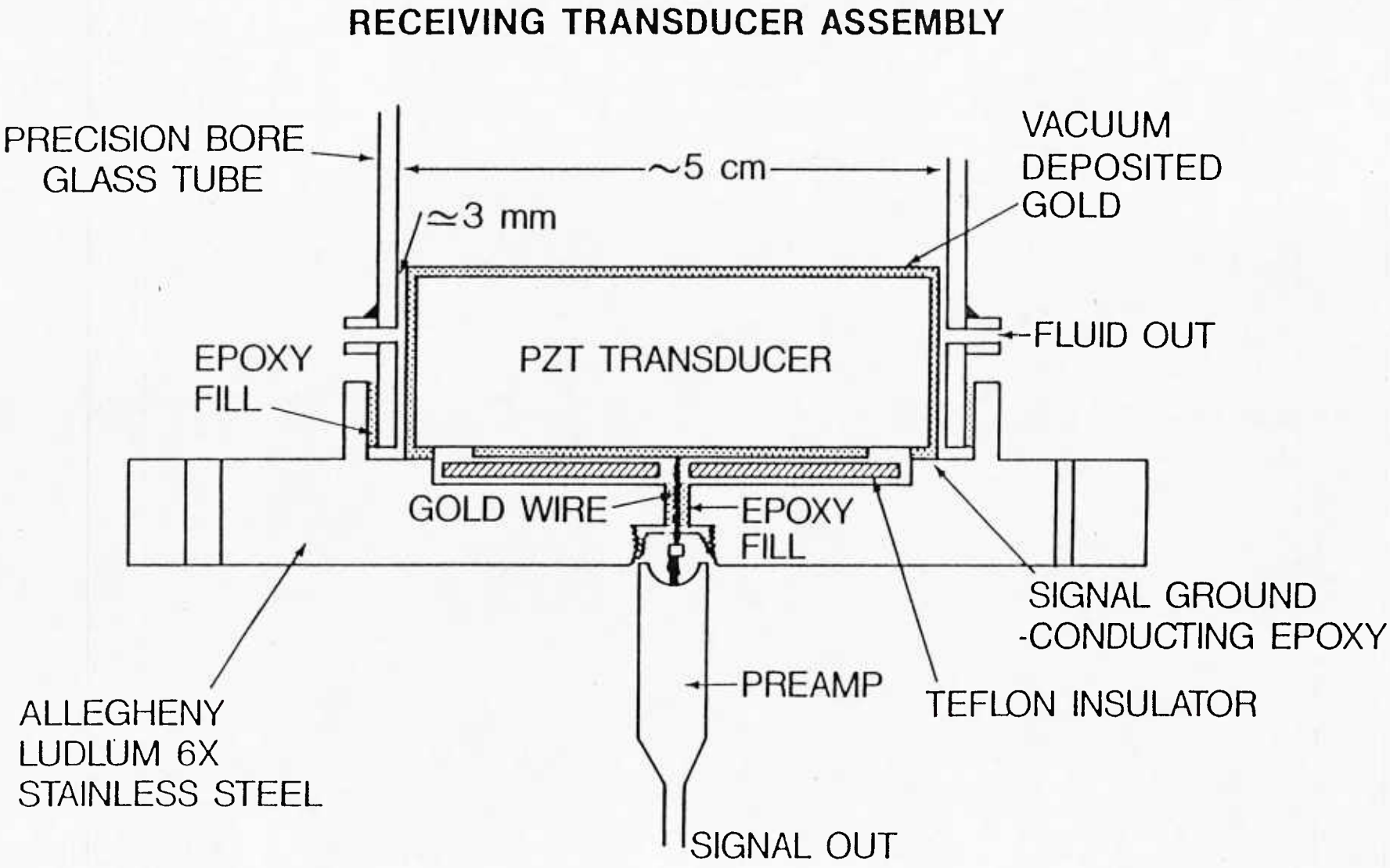
RECEIVING TRANSDUCER ASSEMBLY
PRECISION BORE
GLASS TUBE
~5 cm
VACUUM
DEPOSITED
GOLD
≃3 mm
FLUID OUT
EPOXY
FILL
PZT TRANSDUCER
GOLD WIRE
EPOXY
FILL
SIGNAL GROUND
-CONDUCTING EPOXY
PREAMP
TEFLON INSULATOR
ALLEGHENY
LUDLUM 6X
STAINLESS STEEL
SIGNAL OUT

Figure 2.2

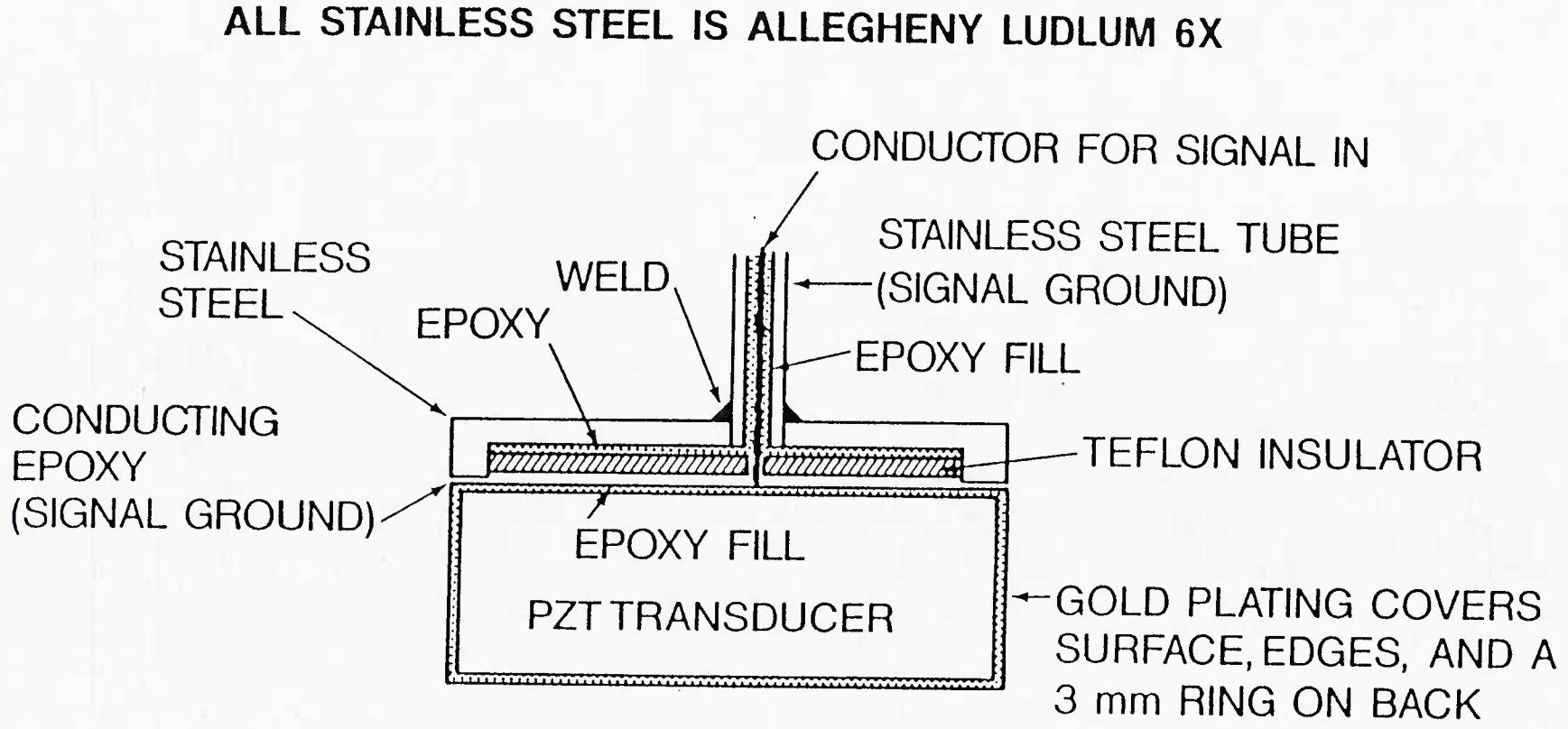
ALL STAINLESS STEEL IS ALLEGHENY LUDLUM 6X
CONDUCTOR FOR SIGNAL IN
STAINLESS STEEL TUBE
(SIGNAL GROUND)
STAINLESS
STEEL
WELD
EPOXY
EPOXY FILL
CONDUCTING
EPOXY
(SIGNAL GROUND)
TEFLON INSULATOR
EPOXY FILL
PZT TRANSDUCER
GOLD PLATING COVERS
SURFACE, EDGES, AND A
3 mm RING ON BACK

Figure 2.3

generated by a variable frequency oscillator (tone burst generator) - amplifier combination. The burst of sine waves (approx. 5 cycles at 93 KHz, 100 cycles at 1 MHz) can be detected by the receiving transducer.

The received signal is preamplified, amplified and filtered before it is fed into an oscilloscope where the amplitude is measured.

2.2 Experimental Results

The earlier measurements indicate that a 20 gm/liter solution of 14K PEO in water will provide an attenuation of 2.8 ± 0.5 dB/m at 630 KHz. The new instrument, then, should be capable of measuring attenuation to an accuracy of ± 0.5 dB/m from below 100 KHz to at least 630 KHz (to provide overlap with previous measurements). In order to test accuracy, a series of measurements was conducted in distilled water. The results are given in Table 2.1. As can be seen, the standard deviation (σ) is an order of magnitude lower than the maximum acceptable value demonstrating that this system is capable of the required accuracy.

Measured Absorption in Distilled Water
(Average of Five Measurements)

Freq. (KHz)	α(dB/m)	σ(dB/m)
91	0.028	0.038
172	0.012	0.008
508	0.024	0.052
851	0.014	0.018
1191	0.004	0.016

Table 2.1

2.3 Status of Research

Measurements are now underway in PEO. All measurements and analyses are scheduled to be competed by the end of this year, when this sub-task will be terminated.

2.4 References

1. "Chemically Induced Acoustic Attenuation," by Brenda Little, Bert Green, O. John Jacobus, and Henry Bass, Final Report, October, 1985.

3.0 The Propagation of Sound in Vibrationally Excited Gases (SACER)

3.1 Summary of Past Work

Bauer and Bass predicted in 1973 the amplification of sound in a gas with an over-population of vibrationally excited states and named the effect "SACER" (sound amplification from controlled excitation reactions)[1]. Calculations were made in 1984 [2] of the magnitude of the effect in a number of gases where the relaxation was slow enough to allow the propagation of a sound wave in the excited gas. During the past year, the results of measurements demonstrating the phenomena in N_2/H_2 mixtures were published,[3] and initial measurements in N_2/He and N_2/CH_4 mixtures were reported.[4] Measurements have also now been made on N_2/H_2O mixtures. Because the relaxation times in these mixtures vary widely, both in magnitude and temperature dependence, this series of measurements serves as a strenuous test of the theory.

Initial measurements have also now been made on CO/H_2 mixtures. For these mixtures an effort will be made to monitor the decay of the vibrational temperature of the CO by the infrared emitted by the excited gas.

3.2 Experimental Method

The experimental equipment is diagrammed in ref. 3. An abrupt electrical discharge through the gas contained in a tube 2.54 cm in diameter and about 30 cm long leaves the gas in a vibrationally excited state and produces a resonant acoustical vibration in the tube. The sound velocity, and hence the translational temperature in the gas, is determined by the change in frequency of the oscillations and the sound absorption (or amplification) is determined from the change in amplitude of the oscillations. Samples of the decaying acoustical oscillations are shown in Fig. 3.1.

In all of the mixtures except N_2/H_2O, the mixtures were prepared and stored in a supplemental tank. For N_2/H_2O mixtures the desired concentration was obtained by bubbling

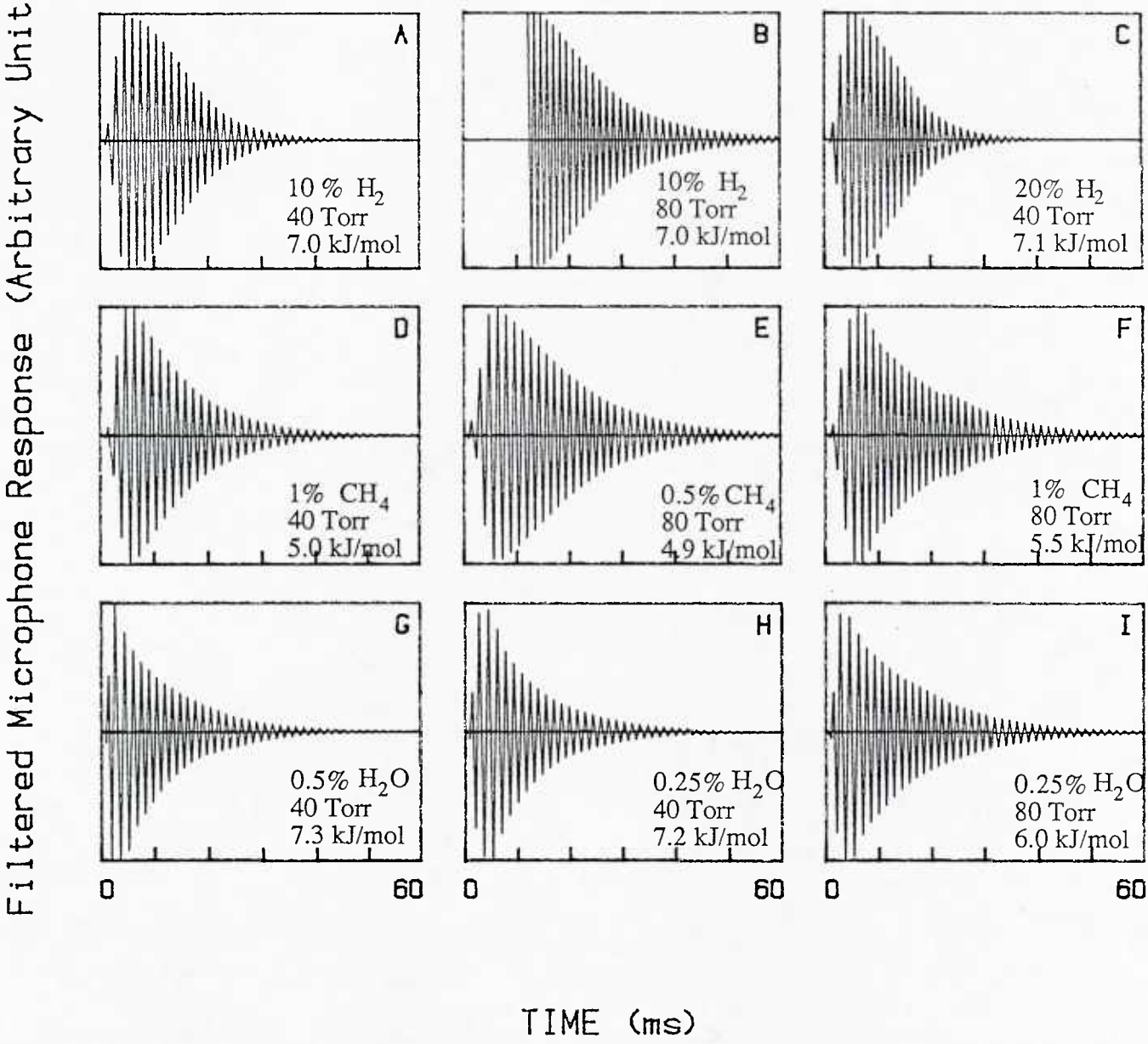

Figure 3.1 Decay of acoustical oscillation in vibrationally excited mixtures of N_2 with H_2, CH_4 and H_2O. The concentrations, gas pressures and initial excess energy in vibration is shown on each figure.

the N_2 through an ice water trap at the pressure needed for the specific concentration. The mixture was allowed to flow through the sound tube until water vapor concentration had equilibrated with the tube wall.

The measured sound velocity is corrected for the tube wall loss and then used to determine the variation of the translational temperature with time following the electrical discharge. Some of these temperature vs. time curves are shown plotted as points in Fig. 3.2.

In order to analyze the results it is desirable to know the initial vibrational temperature and its decay rate. In N_2 mixtures, the initial T_v is obtained by measuring energy deposited in the gas by the discharge and assuming that practically all of this energy goes initially into molecular vibration. For this purpose the voltage pulse across the tube and the current pulse through the tube are measured and stored by a digital oscilloscope. The energy is determined by integrating the product of these curves. The discharge lasts approximately 250 μseconds, and the storage scope samples at a 0.5 μsec rate. The decay of the vibrational temperature is inferred from the measured time dependence of the translational temperature using the relaxation model discussed below.

For the case of CO mixtures it should be possible to get a direct measure of the vibrational temperature as a function of time from a measure of the infrared radiated by the excited gas. For this purpose a CaF_2 window has been mounted on the end of the discharge tube and the radiation coming out of the tube focused on a photo detector. To date the decay of the infrared has been observed but the technique for extracting an absolute temperature measurement from it has not been perfected. Difficulty has also been encountered in getting enough energy into the CO gas from the electrical discharge. The CO seems to have greater conductivity and the present transformer is not capable of delivering enough current. Though theoretical calculations indicate that CO should be similar to N_2, it may be that more of the discharge energy is going into ionization in the CO.

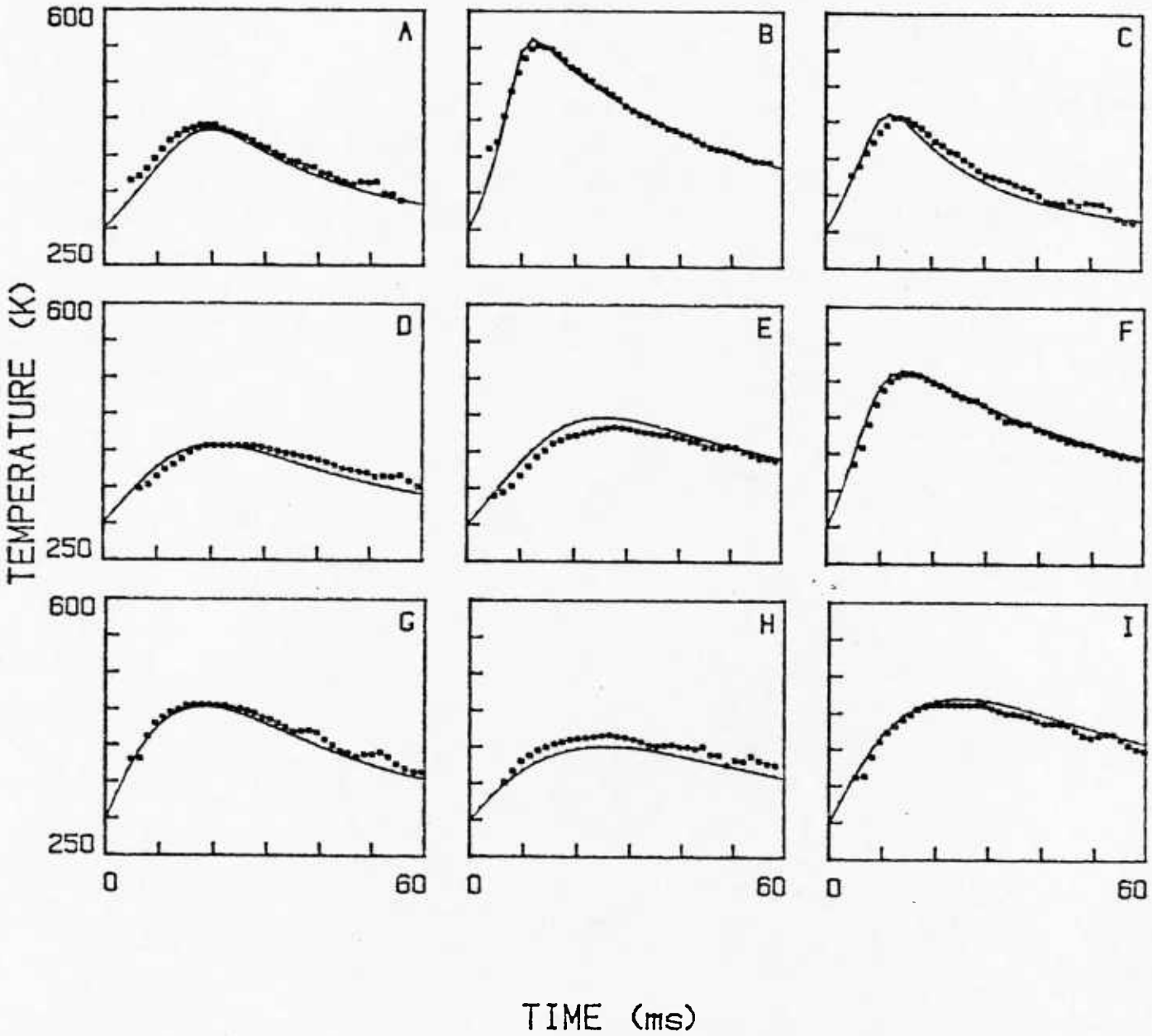

Figure 3.2 Variation of the translational temperature in the gas mixtures shown in Fig. 3.1. The points were calculated from the sound frequencies obtained from the pulses in Fig. 3.1. The curves were calculated as explained in the text.

During the past summer a four channel digital scope has been acquired which allows the simultaneous storage of the discharge voltage, the discharge current, the infrared decay, and the acoustic decay.

3.3 Analysis of the Results

The experimental translational temperature (the points in Fig. 3.2) have been compared to curves calculated from the following relaxation model:

$$\begin{array}{ccc} & \overset{\tau_{vc}}{} & \\ & E_v \longrightarrow \text{wall} & \\ \tau_v & \downarrow & \\ & E_t \longrightarrow \text{wall} & . \\ & \underset{\tau_{tc}}{} & \end{array}$$

Here the vibrational energy is assumed to decay with the passage of energy into translation and to the tube wall with characteristic decay times of τ_v and τ_{vc} respectively. The translational (and rotational) energy is then conducted to the tube wall with a decay time, τ_{tc}. This τ_{tc} has been calculated according to the equation

$$\tau_{tc} = \frac{R^2 \rho C_v K}{2.4^2 \lambda}, \tag{3.1}$$

where R is the tube radius, C_v is specific heat at constant volume, ρ is gas density and λ is the thermal conductivity, and K is an emperical constant. One would expect τ_{vc}/τ_{tc} to equal a constant, but until now little has been determined about the value of that constant. During the past year, considerable time has been spent in trying to improve the method of fitting this relaxation model to the experimental curves shown in Fig. 3.2 and in fitting the gains calculated by the equations of reference 2 with the measured gains. These efforts include the following:

1. The temperature dependence of the vibrational specific heat has been included in the relaxation equations (Eq. 2 of Ref. 4).
2. The two channel oscilloscope has been replaced with a four channel one to allow for the simultaneous measurement of the discharge energy and acoustic pulse.

3. Changes have been made to avoid overdriving the microphone. This is the most important change to date. The 1 inch B&K microphone that was in use last year was being over driven. This evidently was the cause for some of the very large initial gains that were observed following the electrical discharge. The 1 inch microphone has been replaced by a 1/2 inch microphone and care has been taken to make sure it is not over driven. The gains being measured with this microphone are still larger than theory but are now of the same order of magnitude.

4. Previous measurements made with the 1 inch microphone have been repeated with the 1/2 inch microphone.

5. Using the reasoning involved in deriving the Euchen expression,

$$\frac{k}{\eta c_v} = \frac{9\gamma - 5}{4},$$

it has been shown that

$$\tau_{vc}/\tau_{tc} = 1 + 2.25\ R/C_\infty\,, \tag{3.2}$$

where k is thermal conductivity, η is viscosity, c_v is specific heat at constant volume, γ is c_p/c_v, R is the gas constant and C_∞ is the non-relaxing part of the specific heat which in the case of diatomic gas is 5/2 R. This is an important result and has been verified by the curves in Fig. 3.2.

6. The effect of the modulation produced by the sound wave upon the rate at which heat is conducted to the tube wall has been included in the equations used to get the sound amplification. This does not significantly effect the calculated gains.

Through these efforts it has been possible to fit the translational temperature curves (Fig. 3.2) in all of the mixtures with a single adjustable parameter (the K in Eq. 3.1 is set equal to 0.7). Equation 3.1 is derived assuming that the temperature distribution across the tube varies as the zero order Bessel function with the first root at the tube wall. This assumption is certainly invalid for times soon after the discharge. The 0.7 value for K is, therefore, reasonable. The fact that all of the data can be fit by a single adjustable parameter is especially impressive since the relaxation times for N_2 in the various mixtures varies by a factor of 1400 and the rate of change of τ_v with temperature varies by two orders of magnitude.

Having established the value of K in Eq. 3.1 and the validity of Eq. 3.2, it is now possible to extract relaxation times as a function of temperature from the curves in Fig. 3.2. In this way we have determined that the relaxation time for N_2 in water vapor is essentially independent of temperature (a point previously contested) and that an earlier reported room temperature value is 20% too large. This information is needed in predicting sound absorption in air at low humidities and high temperatures.

While some progress has been made in getting agreement between measured and calculated amplification coefficients, the measured values are still larger than expected. This is especially true in N_2/H_2O mixtures. Something maybe going on that is yet not understood. Work continues in trying to understand these differences.

3.4 Work Planned for the Coming Year

The results of the measurements in N_2/He, N_2/CH_4, and N_2/H_2O should be submitted for publication before the end of the year.

In order to predict the SACER effect it is necessary to know the vibrational temperature. At present, as explained above, this vibrational temperature is only inferred from the energy in the discharge and the variation of the translational temperature. It will greatly aid in understanding the experimental results if this vibrational temperature can be measured directly. Initial efforts have been made to do this using CO/H_2 mixtures. These efforts will continue. In addition, an effort will be made to add trace amounts of an infrared active gas (perhaps CO or CO_2) to the N_2 mixtures that are strongly UV coupled to the N_2. In this way the infrared radiation from the trace gas will follow the decay of the N_2 vibrational temperature.

While these experiments were begun in an effort to observe SACER, the phenomena is now well enough understood that it can be used to measure transition rates and their temperature dependencies that are otherwise hard to determine. For example, there is considerable uncertainty in the temperature dependence of the N_2/H_2O relaxation time. This information is needed in order

to calculate sound absorption in both N_2 and air at high temperatures and low humidities. The measurements recently completed should provide valuable information about these rates.

As time permits, an effort will be made to observe SACER in polyatomic gases. In this case, the sound will be high frequency and the vibrational excitation will be produced by irradiating the gas with a high intensity pulse of laser light. This experiment would extend into 1989.

References

1. H.J. Bauer and H.E. Bass, Phys. Fluids 16, 988 (1973).
2. F. Douglas Shields, J. Acoust. Soc. Am. 76, 1749 (1984).
3. F. Douglas Shields, J. Acoust. Soc. Am. 81, 87 (1987).
4. F. Douglas Shields and L. Dwynn Lafleur, J. Acoust. Soc. Am., Suppl. 1, 80, S120 (1986).